NIH Public Access
Author Manuscript
Biochemistry. Author manuscript; available in PMC 2014 June 04.

Published in final edited form as:
Biochemistry. 2013 June 4; 52(22): 3921–3929. doi:10.1021/bi400295x.

Modification of inter-domain interfaces within the A3C1C2 subunit of factor VIII affects its stability and activity

Hironao Wakabayashi and **Philip J. Fay***
Department of Biochemistry and Biophysics, University of Rochester School of Medicine, 601 Elmwood Ave., Rochester, NY 14642, USA

Abstract

Factor (F)VIII consists of a heavy chain [A1(a1)A2(a2)B domains] and light chain [(a3)A3C1C2 domains]. Several reports have shown significant changes in FVIII stability and/or activity following selected mutations at the interfaces of the A1-A2, A1-A3, A2-A3, or A1-C2 domains. In this study the remaining inter-FVIII subunit interfaces (A3-C1 and C1-C2) were examined for their contributions to FVIII/FVIIIa stability and activity. We prepared FVIII mutants with a nascent disulfide bridges between A3 and C1 domains (Gly1750Cys/Arg2116Cys and Ala1866Cys/Ser2119Cys) or C1 and C2 domains (Ser2029Cys/Pro2292Cys). We also prepared mutants replacing Arg2116 with hydrophobic residues (Ala and Val) since this C1 domain residue appears to face a pocket of positive electrostatic potential in the A3 domain. Stability was assessed following the rates of loss of FVIII activity at 55°C and the spontaneous loss of FVIIIa activity from A2 subunit dissociation. FVIII Gly1750Cys/Arg2116Cys showed a marked increase in thermal stability (~3.7 fold) as compared with WT FVIII while the stability of FVIII Ala1866Cys/Ser2119Cys was reduced (~4.7 fold). Although the Ser2029Cys/Pro2292Cys variant showed a modest loss in FVIII stability, the specific activity and thrombin generation potential of this variant were increased (up to 1.2-fold) compared with WT. Furthermore, this variant demonstrated an ~2-fold reduced K_m for FX. Mutation of Arg2116 to hydrophobic residues resulted in variable decreases in stability and thrombin generation parameters suggesting a role of this Arg residue contributing to FVIII structure. Taken together, selective modification of the contiguous domain interfaces in FVIII light chain may improve FVIII stability and/or cofactor function.

Factor (F) VIII, a plasma protein that is decreased or defective in individuals with hemophilia A, is expressed as both single chain and heterodimer forms. The latter consists of a heavy chain (HC) comprised of A1(a1)A2(a2)B domains and a light chain (LC) comprised of (a3)A3C1C2 domains, with the lower case *a* representing short (~30-40 residue) segments rich in acidic residues (see Ref.[1] for review). FVIII is activated by proteolytic cleavages at the a1A2, a2B and a3A3 junctions catalyzed by thrombin or factor Xa. The resulting product, FVIIIa, is a heterotrimer comprised of subunits designated A1, A2, and A3C1C2 that functions as a cofactor for the serine protease FIXa in the membrane-dependent conversion of zymogen FX to the serine protease, FXa (see Ref.[1] for review).

Reconstitution studies have shown that the FVIII heterodimeric structure is supported by both electrostatic and hydrophobic interactions[2]. Metal ions also contribute to the inter-chain affinity and activity parameters[3]. Occupancy of a calcium site in the A1 domain (110-126) is required to yield the active FVIII conformation[4]. Copper ions facilitate the association of HC and LC to form the heterodimer, increasing the inter-chain affinity by several-fold at

*Corresponding Author Department of Biochemistry and Biophysics, University of Rochester School of Medicine, 601 Elmwood Ave., Rochester, New York, 14642, Phone: 585-275-6576 philip_fay@urmc.rochester.edu.

The authors declare no competing financial interest.

NIH-PA Author Manuscript
NIH-PA Author Manuscript
NIH-PA Author Manuscript

NIH-PA Author Manuscript
NIH-PA Author Manuscript
NIH-PA Author Manuscript

physiologic pH[5,6]. Intermediate resolution X-ray structures of FVIII[7,8] showed occupancy of a calcium site in the A1 domain and the two type 1 copper ion sites within the A1 and A3 domains.

The instability of FVIIIa results from weak electrostatic interactions between the A2 subunit and the A1/A3C1C2 dimer[9,10] and its dissociation leads to dampening of FXase activity[11,12]. Examination of hydrogen-bonding interactions at the A1-A2 and A2-A3 interfaces following mutation of selected charged/polar residues spatially separated by <2.8 Å showed loss of function, as judged by increased rates of FVIII decay at 55°C and/or rates for FVIIIa decay relative to WT, in approximately half of the 30 residues tested[13], suggesting that multiple residues at the A1-A2 and A2-A3 domain interfaces contribute to the stabilization of FVIII.

Mutations to increase buried hydrophobic area and/or reduce the buried hydrophilic area often results in enhanced protein stability[14]. Earlier studies showed that acidic residues localized to hydrophobic pockets at the A1-A2 interface (Asp519) and A2-A3 interface (Glu665 and Glu1984) when mutated to hydrophobic residues (Ala or Val), yielded favorable effects on FVIII/FVIIIa stability and/or activity[15,16]. In addition, replacing Ala108 that localized to a hydrophobic pocket at the A1-C2 domain interface with the more bulky Ile also showed a marked increase in FVIII stability[17]. Furthermore, introducing nascent disulfide bridges between FVIII subunits by double Cys mutation at A2-A3 or A1-C2 interfaces yielded FVIII variants with enhanced FVIII/FVIIIa stability[17-19].

Although the A3C1C2 domains are covalently linked in FVIII light chain, the FVIII X-ray crystal structure suggests the A3-C1 and C1-C2 domain interfaces are maintained by non-covalent interactions[7,8]. In this study we examined the effect of generating additional covalent and non-covalent interactions at the A3-C1 and C1-C2 interfaces. Results show that a selected A3-C1 interface modification is favorable for FVIII stability and C1-C2 interface modification enhanced cofactor function likely by reducing the K_m of FXase for substrate factor X. In addition these result reveal a role for C1 residue Arg2116 in maintaining FVIII stability.

MATERIALS AND METHODS

Reagents

Recombinant FVIII (Kogenate™) and the monoclonal anti-A3 antibody 2D2 were generous gifts from Dr. Lisa Regan of Bayer Corporation (Berkeley, CA). Phospholipid vesicles containing 20% phosphatidylcholine (PC), 40% phosphatidylethanolamine (PE), and 40% phosphatidylserine (PS) were prepared using octylglucoside as described previously[20]. The reagents α-thrombin, FVIIa, FIXaβ, FX, and FXa (Enzyme Research Laboratories, South Bend, IN), hirudin and phospholipids (DiaPharma, West Chester, OH), the chromogenic FXa substrate, Pefachrome Xa (Pefa-5523, CH_3OCO-D-CHA-Gly-Arg-pNA·AcOH; Centerchem Inc. Norwalk CT), recombinant human tissue factor (rTF), Innovin (Dade Behring, Deerfield, IL), fluorogenic substrate, Z-Gly-Gly-Arg-AMC (Calbiochem, San Diego, CA), thrombin calibrator (Diagnostica Stago, Parsippany, NJ) and Enhanced Chemifluorescence reagent (GE Healthcare Bioscience,Piscataway, NJ) were purchased from the indicated vendors.

Construction, Expression and Purification of WT and Variant FVIII

WT FVIII and variants with double mutations (Gly1750Cys/Arg2116Cys, Ala1866Cys/Ser2119Cys, and Ser2029Cys/Pro2292Cys) and single mutations (Arg2116Ala and Arg2116Val) were individually constructed as B domainless FVIII, lacking residues Gln744-Ser1637 in the B-domain[21]. Recombinant WT and variant FVIII forms were stably

NIH-PA Author Manuscript

NIH-PA Author Manuscript

NIH-PA Author Manuscript

expressed in BHK cells and purified as described previously[4]. Protein yields for the variants ranged from >10 to ~100 μg from two 750 cm^2 culture flasks, with purity from ~85% to >95% as judged by SDS-PAGE. The primary contaminant in the FVIII preparations was albumin. FVIII concentration was measured using an Enzyme-Linked Immunoadsorbant Assay (ELISA) and FVIII activity was determined by one-stage clotting and two-stage chromogenic FXa generation assays described below.

ELISA

A sandwich ELISA was performed as previously described[22] using purified commercial recombinant FVIII (Kogenate, Bayer Corporation) as a standard. FVIII capture used the anti-C2 antibody (GMA8003, Green Mountain Antibody, Burlington, VT) and the R8B12 antibody (Green Mountain Antibody) was employed for FVIII detection following its biotinylation.

FVIII Activity and Stability Measurements

One-stage clotting assays were performed using substrate plasma chemically depleted of FVIII as previously described[15]. The rate of conversion of FX to FXa was monitored in a purified system according to a two-stage FXa generation assay previously described[15]. FVIII activity decay at elevated temperatures (55°C) was measured by incubating WT or variant FVIII (4 nM) in 20 mM N-[2-hydroxyethyl]piperazine-N'-[2-ethanesulfonic acid] (HEPES), pH 7.2, 0.1 M NaCl, 0.01% bovine serum albumin, 0.01% Tween 20 (buffer A) and monitoring residual FVIII activity using a FXa generation assay. The spontaneous decay of FVIIIa activity was measured following activation of WT or mutant FVIII (1.5 nM) by thrombin (20 nM) for 1 min in the absence or presence of FIXa (10nM) with followed by addition of hirudin (10 U/ml) to inactivate thrombin. Residual activity was determined using the FXa generation assay. Data were fitted to the single exponential decay equation by non-linear least squares regression and parameter values were obtained.

Michaelis-Menten Kinetics and FIXa Binding Affinity

FVIII (1 nM) in buffer A containing 10 μM PSPCPE vesicles was activated by 20 nM thrombin for 1 min, immediately reacted with hirudin (10 U/ml) and 40 nM FIXa and FXa generation was initiated by adding the indicated concentrations of FX. Measurement of the binding affinity of FVIIIa for FIXa was performed as follows. FVIII (1 nM) in buffer A containing 10 μM PSPCPE vesicles was activated by 20 nM thrombin for 1 min, immediately reacted with hirudin (10 U/ml) and the indicated concentrations of FIXa, and FXa generation was initiated by adding 300 nM FX as described above. Data were fitted to the Michaelis-Menten equation or the steady state binding equation by non-linear least squares regression and parameter values were obtained.

Western blotting

FVIIIa proteins prepared following activation of FVIII (0.34 μg) by thrombin (20 nM) for 30 min at 23°C were subjected to electrophoresis under reducing (0.1 M dithiothreitol) and non-reducing conditions using 6% polyacrylamide gels at constant voltage (150V). Proteins were transferred to a polyvinylidene fluoride membrane, probed with an anti-A3 domain monoclonal antibody (2D2) and protein bands were visualized by chemifluorescence using a Gel Doc™ XR+ System (Bio-Rad, Hercules, CA).

Thrombin Generation Assay

The amount of thrombin generated in plasma was measured by Calibrated Automated Thrombography[23] using methods previously described[15]. Briefly, FVIII deficient plasma (<1% residual activity, platelet-poor) from a severe hemophilia A patient lacking FVIII

NIH-PA Author Manuscript

NIH-PA Author Manuscript

NIH-PA Author Manuscript

inhibitor (George King Bio-Medical, Overland Park, KS) was mixed at 37°C with a final concentration of 0.25 nM FVIII, 0.5 pM rTF, 4 μM PSPCPE vesicles, 433 μM fluorogenic substrate, 13.3 mM $CaCl_2$, and 105 nM thrombin calibrator. The development of a fluorescence signal was monitored at 8 second intervals using a Microplate Spectrofluorometer (Spectramax Gemini, Molecular Devices, Sunnyvale, CA) with a 355 nm (excitation)/460 nm (emission) filter set. Fluorescence signals were corrected by the reference signal from the thrombin calibrator samples[23] and actual thrombin generation in nM was calculated as previously described[15].

Data Analysis

FVIII/VIIIa activity values as a function of time were fitted to a single exponential decay curve by non-linear least squares regression using the equation,

$$A = A_0 \cdot e^{-k \cdot t}$$

where A is residual FVIIIa activity (nM/min/nM FVIII), A_0 is the initial activity, k is the apparent rate constant, and t is the time (minutes) of reaction of either FVIII at 55°C (for FVIII decay experiments) or after thrombin activation was quenched (for FVIIIa decay measurements). For Michaelis Menten-kinetics or FIXa binding affinity measurements we used the following equation,

$$A = \frac{V_{\max} \cdot X}{K + X}$$

where A is initial velocity of FXa generation (nM/min/nM FVIII), X is the FX or FIXa concentration, K is the Michaelis constant (K_m) or dissociation constant (K_d), and V_{max} is the maximum activity at saturating substrate.

Nonlinear least-squares regression analysis was performed using a standard curve-fitting algorithm (Gauss-Newton algorithm with Levenberg-Marquardt method). Comparison of average values was performed by the Student's *t*-test.

RESULTS

Generation of FVIII variants with nascent disulfide bridging at the A3-C1 and C1-C2 domain interfaces and point mutants at Arg2116

The A3C1C2 subunit of FVIIIa is a single chain protein with domains delineated by residues Lys2020-Cys2021 (A3-C1) and Cys2169-Asp2170 (C1-C2) (see Fig. 1). In addition to covalent attachment, the inter-domain interfaces show potential for significant non-covalent interactions. Figure 1A illustrates the A3-C1 interface and identifies two residues, Ala1866 and Gly1750 in the A3 domain that are in close proximity to C1 domain residues Ser2119 and Arg2116, respectively (Cα distances of 6.5 Å and 5.4 Å, respectively[8]). In an attempt to increase stability to this region, these paired residues (Ala1866/Ser2119 and Gly1750/Arg2116) were mutated to Cys to form additional covalent linkages through nascent disulfide bonding. In addition, we noted that the C1 residue Arg2116 resides at the inter-domain interface in close proximity to an area of basic electrostatic potential in the A3 domain. Since this interaction could be destabilizing to A3-C1 domain interactions, we mutated this residue to either Ala or Val. Finally, examination of the C1-C2 domain interface (Fig 1B) indicated a close proximity of C1 domain residue Ser2029 with C2 domain residue Pro2292 (Cα distance of 7.3 Å[8]) and these residues were mutated to Cys in an effort to disulfide bridge the two C domains. While the above FVIII variants could be

NIH-PA Author Manuscript

NIH-PA Author Manuscript

NIH-PA Author Manuscript

expressed in BHK cells, we noted that other pairings attempted to produce disulfide bridges linking A3 and C1 domains (Glu1751Cys/Pro2142Cys, Leu1752Cys/Asn2118Cys, Leu1752Cys/Pro2142Cys, His1867Cys/Ser2119Cys, and Val1933Cys/Pro2143Cys) or C1-C2 domains (Ser2029Cys/Val2293Cys and Ser2029Cys/Val2294Cys) were not expressed in cell culture.

Specific activity values of purified FVIII proteins were measured by both one-stage and two-stage assays and data are shown in Table 1. FVIII Gly1750Cys/Arg2116Cys retained ~60% specific activity of FVIII WT, whereas that of Ala1866Cys/Ser2119Cys was reduced to ~30% the WT value. The C1-C2 interface mutant (Ser2029Cys/Pro2292Cys) and the point mutants Arg2116Ala and Arg2116Val possessed specific activity values near the WT value.

Formation of disulfide bonds was assessed by comparison of the electrophoretic mobility of the variants compared with WT A3C1C2. Fig. 2 shows SDS-PAGE of the A3C1C2 subunits of WT FVIII and variants as detected by an anti-A3 domain monoclonal antibody (2D2). Under reducing conditions (0.1 M dithiothreitol), WT and variant A3C1C2 subunits showed equivalent mobility migrating to the same position (~70 kDa, lanes 1-4) on the gel. However, under non-reducing conditions the A3C1C2 subunits from the disulfide-bridged variants Gly1750Cys/Arg2116Cys (lane 6), Ala1866Cys/Ser2119Cys (lane 7), and Ser2029Cys/Pro2292Cys (lane 8) migrated faster than WT A3C1C2 (lane 5). These results are consistent with the presence of an additional covalent bridge in the subunit yielding a tighter inter-subunit conformation.

Stability of FVIII variants

FVIII thermal decay assay at 55°C as measured by FXa generation assay represents the stability of inter-subunit interaction (6). Fig. 3 shows the results of thermal decay at 55°C for the FVIII WT and variants. Among the mutants tested only Gly1750Cys/Arg2116Cys showed an increased thermal stability retaining ~70% activity at ~35 min after heat-challenge as compared with WT, which was reduced to <70% activity in 10 min (Fig. 3A). The calculated decay rate for this variant was reduced by ~3.6 fold compared with the FVIII WT value (Table 1) and this result is consistent with the additional disulfide bridge at the A3-C1 interface stabilizing the FVIII structure. Alternatively, the Ala1866Cys/Ser2119Cys variant, which also possesses an added disulfide bridge at this interface, yielded a faster decay than WT with <20% activity remaining in 10 min (Fig. 3A). The calculated decay rate for this variant was ~4.7 fold greater than the WT value (Table 1). These results indicate markedly different effects on FVIII stability dependent upon the location of the added linkage within the A3-C1 interface. FVIII variants with point mutations at Arg2116 showed faster thermal decay rates as compared with WT with the Arg2116Ala yielding an ~5-fold increase in rate while the Arg2116Val yielded a nearly 2-fold increase in rate (Fig. 3A and Table 1). These results indicate that the Arg residue at this site in native FVIII likely contributes favorable interaction(s) to FVIII structure in stabilizing the domain interface, whereas the hydrophobic Ala or Val at this position is destabilizing. The decay rate of C1-C2 interface mutant (Ser2029Cys/Pro2292Cys) was also faster than WT, showing ~20% activity remaining after 10 min at the elevated temperature (Fig. 3A), which was estimated to be an ~3.7-fold increase as compared with WT FVIII (Table 1).

FVIIIa activity decay is governed by the dissociation of the A2 subunit, which interacts with the A1 subunit and A3 domain of the A3C1C2 subunit. Since these interactive sites are far removed from the A3-C1 and C1-C2 domain interfaces, we did not expect to observe large changes in FVIIIa stability with the variants. Although modest, the Gly1750Cys/Arg2116Cys variant possessed an improved FVIIIa stability showing an activity value retaining 5-10% more than WT after 10 min incubation (Fig. 3B). The estimated FVIIIa

NIH-PA Author Manuscript

NIH-PA Author Manuscript

NIH-PA Author Manuscript

decay rate for this variant was ~30% slower than WT FVIII (Table 1, $p < 0.05$). Interestingly in the presence of FIXa (10 nM) the FVIIIa decay rate was lower but similar to WT FVIII (Table 1), suggesting that the effect of this mutation of FVIIIa stability can be substituted by FIXa. FVIIIa decay profiles for the Ala1866Cys/Ser2119Cys variant and the two Arg2116 mutants were similar to WT in the absence of FIXa and the value was lower and approached the WT value in the presence of FIXa (Table 1). Thrombin activated Ser2029Cys/Pro2292Cys FVIIIa decayed slightly faster than WT FVIIIa showing an ~1.2 fold increase in decay rate as compared with WT, however, in the presence of FIXa the decay rate was ~1.2 fold lower than the WT value (Table 1). The above data suggest that modifications at the interface of A3-C1 and C1-C2 domains result in generally minimal effects relative to A2 subunit retention.

Thrombin generation

FVIII variant activity was assessed by thrombin generation assays performed at low rTF concentration (0.5 pM) using FVIII deficient plasma. Fig. 4 shows a representative thrombogram of FVIII WT and selected variants with parameter values listed in Table 2. Thrombin generation of WT FVIII initiated at ~12 min and peak thrombin generation (~110 nM) was reached at ~19 min. The FVIII Gly1750Cys/Arg2116Cys and Ala1866Cys/Ser2119Cys variants showed reductions in thrombin generation with ETP values 54% and 43% the WT value, respectively. These values were compatible with the observed specific activity values (~60% and 30%, respectively) for the two variants. Furthermore, we observed a significant delay for thrombin generation parameters (~10% in latent time and ~30% in peak time relative to WT) for the Ala1866Cys/Ser2119Cys variant. On the other hand, the Ser2029Cys/Pro2292Cys variant linking C1 and C2 domains showed somewhat improved thrombin generation (112% ETP value as compared with WT FVIII value, $p < 0.05$), which again corresponded to the increased specific activity (117% by one-stage assay) of this variant. Furthermore, latent and peak times were significantly shortened (~20 and 35%, respectively) relative to WT. Thrombin generation using the Arg2116 Ala and Val mutants showed ~30% reductions in peak and ETP values compared with WT values. In addition, we performed experiments to measure thrombin activation of FVIII under conditions where excess FVIII (20 nM) was activated by 0.5 nM thrombin and the rate of FVIIIa generation was measured as an initial velocity during a 1 min reaction in 10 second intervals. All of the mutants showed similar efficiency as compared with WT FVIII (within 20% difference). The rate values were 34.7 ± 0.69, 36.1 ± 1.21, 33.6 ± 1.16, 41.3 ± 2.70, and 33.6 ± 1.89 nM FVIIIa generated per min per nM thrombin for WT FVIII, Gly1750Cys/Arg2116Cys, Ala1866Cys/Ser2119Cys, Arg2116Ala, and Arg2116Val, respectively. Furthermore, the FVIII WT and variants show similar affinity values for FIXa (within 10% difference). K_d values were 0.43 ± 0.02, 0.44 ± 0.05, 0.40 ± 0.04, 0.45 ± 0.05, and 0.40 ± 0.06 nM for WT FVIII, Gly1750Cys/Arg2116Cys, Ala1866Cys/Ser2119Cys, Arg2116Ala, and Arg2116Val, respectively. Overall, the reason for modestly reduced thrombin generation profile of the Arg2116 mutants is not clear, but may reflect the slightly increased FVIIIa decay rate observed in the absence of FIXa.

FVIII function analyses of WT and Ser2029Cys/Pro2292Cys variants

In order to gain insights into the increased specific activity (by one-stage assay) and thrombin generation potential of the Ser2029Cys/Pro2292Cys variant relative to WT, we examined functional interactions of the cofactor with FIXa and FX. For interactions with FIXa, FVIII (1nM) WT or variant was activated by thrombin, titrated with various concentrations of FIXa, and rates of FXa generation were measured as described in Methods. FXa generation curves for WT and the Ser2029Cys/Pro2292Cys variant were hyperbolic and saturable with FIXa (data not shown). From the fitted curves, K_d values of 0.43 ± 0.02 and 0.33 ± 0.04 nM were determined for WT and the Ser2029Cys/Pro2292Cys

NIH-PA Author Manuscript

NIH-PA Author Manuscript

NIH-PA Author Manuscript

variant, respectively. These results suggest both WT and variant show similar affinity values for FIXa. Thrombin (0.5 nM) activation measurements of FVIII (20 nM) also showed similar values (34.7 ± 0.69 and 38.5 ± 1.11 nM FVIIIa generated per min per nM thrombin) for WT and the Ser2029Cys/Pro2292Cys variant, respectively.

Michaelis-Menten kinetics were used to assess the FVIIIa-dependent interaction of FX with the FXase complex. The rate of generation of FXa with 1 nM FXase (1 nM FVIII activated by thrombin and reacted with 40 nM FIXa) was performed at various concentrations of FX as described in Methods. Results are shown in Fig. 5. Both WT and Ser2029Cys/Pro2292Cys FVIII generated FXa at rates that were saturable showing hyperbolic titration curves as FX concentration increased. The estimated V_{max} values were 44.8 ± 1.3 and 37.8 ± 1.5 nM/min for WT and Ser2029Cys/Pro2292Cys, respectively. Interestingly the K_m value for the mutant was ~ one half the WT value (32.8 ± 2.6 and 16.5 ± 2.4 nM for WT and Ser2029Cys/Pro2292Cys FVIII, respectively, $p < 0.005$). The reduced K_m for FX observed for the disulfide-bridged variant likely contributes in part to the modest increase in activity observed in the one-stage and thrombin generation assays where plasma concentrations of FX are present.

DISCUSSION

Previously we reported that mutagenesis of selected residues at the A1-A2, A2-A3, A1-A3, and A1-C2 domain interfaces variably affected, both positively and negatively, FVIII and/or FVIIIa stability[6,13,16,17,24]. In the current study we extend this line of investigation to the remaining intra-FVIII interactions by examining effects of mutations the A3-C1 and C1-C2 domain interfaces, localized within the single chain A3C1C2 subunit. Results from this study show differential effects when placing an additional covalent linkage, in the form of a nascent disulfide bridge, to the A3-C1 domain interface. Residue pairings for mutagenesis to Cys were chosen based upon residue Cα spatial separations of ~5-7 Å. While the Gly1750Cys/Arg2116Cys variant showed an ~3-4-fold increase in FVIII thermal stability that was accompanied by a modest increase in FVIIIa stability, the Ala1866Cys/Ser2119Cys FVIII variant decayed at a rate nearly 5-times the WT FVIII value at elevated temperature. Thus constraints imposed by the disulfide bonds at this interface show markedly disparate effects. Furthermore, the positive charge of Arg2116 appears to directly contribute to the interface stability based upon reductions in this and other parameters values when this residue is replaced by Ala or Val. Finally, mutation to place a nascent disulfide bridge at C1-C2 interface (Ser2029Cys/Pro2292Cys) resulted in marked reduction in FVIII thermal stability. However, this FVIII variant showed a modest increase in specific activity, possibly as a result of improved interaction of the cofactor with substrate FX.

It is not surprising that one of the mutants (Gly1750Cys/Arg2116Cys) with a nascent disulfide bridge at A3-C1 interface increased FVIII thermal stability. In an earlier study we showed that introduction of a disulfide bridge by the mutation Arg121Cys/Leu2302Cys at the A1-C2 domain interface resulted in a 3-fold reduction in FVIII decay at elevated temperatures relative to WT FVIII[17]. Our current findings suggest that non-covalent interactions at the A3-C1 interface contribute to overall FVIII structural integrity. Thus, applying additional strength to this interaction by creation of a disulfide bridge at this site increased FVIII stability. In addition, the Gly1750Cys/Arg2116Cys variant showed a modest increase in FVIIIa stability. This effect may be explained by observations that the A2 domain interacts with both A1 and A3 domains, and that A3 is supported by both A1 and C1 domains in order to interact optimally with A2 domain. Therefore we speculate that the stabilization of A3 domain relative to C1 domain may cause a favorable effect on A2 domain binding in FVIIIa. However, we also observed that this increase in FVIII stability by fixing the A3-C1 interface appeared characteristic to a specific inter-domain residue pairing

NIH-PA Author Manuscript

NIH-PA Author Manuscript

NIH-PA Author Manuscript

based upon the disparate effects noted for the Gly1750Cys/Arg2116Cys and Ala1866Cys/Ser2119Cys variants. The reason(s) for the low stability of the Ala1866Cys/Ser2119Cys variant is not known but the concurrent low activity of this variant suggests that the nascent disulfide bridge imposed a non-native structural constraint that was detrimental to function.

On the other hand, while the stability of the Ser2029Cys/Pro2292Cys (C1-C2 bridged) FVIII variant was reduced, this variant retained essentially WT-like, if not somewhat increased activity. Thus any global structural change due to mutation was unlikely. It is possible that constraints imposed by the bridging the C1-C2 domain interface caused a negative effect(s) at other, more distal interfaces leading to a loss of stability. We attempted to test this alternative by preparing a FVIII mutant with disulfide bridging at both the A1-C1 domain interface and the C1-C2 interface. That mutation (FVIII Arg121Cys/Leu2302Cys/Ser2029Cys/Pro2292Cys) possessed an efficient linkage between C1 and C2 domains based upon SDS-PAGE. However, there was only partial bridging (<50%) at the A1-C2 interface as judged by free A1 and A3C1C2 subunits compared with the dithiothreitol-resistant A1-A3C1C2 dimer (data not shown). This result was unexpected since the FVIII Arg121Cys/Leu2302Cys variant had previously shown essentially complete disulfide bond formation[17]. This observation suggests that the altered A1-C2 domain interaction that limited bridging in the double disulfide bond variant resulted from a constraint imposed by bridging at the C1-C2 interface. Although limited information could be derived for this variant due to incomplete bridging, the thermal stability of the double-disulfide bridged mutant was reduced to a lesser extent (1.6-fold) relative to WT (results not shown) than was the C1-C2 bridged variant (3.7-fold relative to WT). Thus we speculate that the decreased thermal stability of the C1-C2 bridged variant results from other, more distal alterations such as a possible change at the A1-C2 interface.

Interestingly, adding a disulfide bridge to the C1-C2 domain interface in the FVIII Ser2029Cys/Pro2292Cys variant modestly improved FVIII activity in a one-stage clotting assay and thrombin generation potential but not activity measured in a two-stage FXa generation assay. We speculate these results derive from an enhanced interaction of the variant FVIII with FX. The one-stage clotting and thrombin generation assays use diluted plasma as a source for FX, thus the substrate is not at V_{max} concentration, unlike the two-stage FXase assay that uses purified proteins including a V_{max} concentration of FX substrate. Thus the reduced Km would increase catalytic efficiency of FXase with limiting substrate in the plasma-based assays. Furthermore, affinity values of the WT and Ser2029Cys/Pro2292Cys FVIII variant for FIXa were quite similar. In addition, experiments measuring fluorescence anisotropy of fluorescein-Phe-Phe-Arg FIXa (fl-FFR-FIXa) showed no change in anisotropy values comparing the WT and variant FVIII. However, the increase in anisotropy following addition of FX to FXase complex was somewhat faster for FXase comprised of mutant FVIIIa than that of WT FVIIIa (data not shown), suggesting that the association rate for FX was increased with the variant cofactor. Since the C2 domain is reported to form a part of the binding sites for FXa and FIXa[25-27], it is not surprising that increased structural stabilization of C2-C1 boundary could improve the inter-protein interactions. To our knowledge, this is the first report of the generation of FVIII variant with increased FX affinity.

Results from the mutagenesis of Arg2116 suggest this residue contributes to the binding energy at A3-C1 interface. As suggested by the intermediate resolution (3.98 Å) FVIII X-ray crystal structure[8], the side chain of Arg faces a strong positive charge in the A3 domain from the amide nitrogen from Gly1750 and from the side chain of Arg1749 (Fig. 1, bottom right panel). Thus one would predict this interaction to be destabilizing. However, experimental results eliminating this charge following replacement of Arg2116 with Ala or Val yielded reductions in FVIII stability. These results suggest the presumed location of the Arg2116

NIH-PA Author Manuscript

NIH-PA Author Manuscript

NIH-PA Author Manuscript

side chain may not be accurate. We note that the acidic side chain of Glu1751 appears to be in close proximity to Arg2116 (Cα distance = 6.18 Å). Thus we speculate that the side chain of Arg2116 may be in an appropriate position to accommodate an electrostatic interaction with Glu1751.

Our results from several studies examining FVIII and FVIIIa stability following selected mutation at each domain interface have yielded several general observations. Enhancing the affinity of the A2 subunit of FVIIIa for the A1/A3C1C2 dimer by replacing destabilizing charged residues in hydrophobic pockets at the A1-A2 and A2-A3 domain interfaces shows clear correlations with increased specific activity, thermal stability and thrombin generation parameters[15,16]. These improved activity and thrombin generation values are consistent with earlier studies where A2 domain was covalently linked to other FVIII domains by disulfide bridging[18,19]. On the other hand, modifications to improve stability at interfaces not involving the A2 domain [A1-C2[17], and A3-C1 and C1-C2 (this study)] show variable effects on the thermal stability of FVIII and minimal effects on the decay of FVIIIa. Nascent disulfide bonds with the mutations Arg121Cys/Leu2302Cys (A1-C2)[17], and Gly1750Cys/Arg2116Cys (A3-C1, this study) resulted in ~3-fold reductions in the rate of FVIII decay at elevated temperature, whereas the Ala1866Cys/Ser2119Cys (A3-C1) and Ser2029Cys/Pro2292Cys (C1-C2) variants in this study showed marked decreases in thermal stability. Thus non-native covalent linkages can be clearly detrimental to protein structure. However, we note that conditions used for activity measurements such as specific activity and thrombin generation parameter values, the FVIII thermal stability parameter value does not necessarily correlate with these activity parameters.

Acknowledgments

We thank Lisa M. Regan of Bayer Corporation for the gifts of recombinant human FVIII and anti-FVIII antibody (2D2), and Pete Lollar and John Healey for the FVIII cloning and expression vectors.

Funding

This work was supported by NIH grants HL38199 and HL76213.

ABBREVIATIONS

WT	wild type
FVIII	factor VIII
FX	factor X
FIXa	factor IXa
FXase	factor Xase
SDS-PAGE	sodium dodecyl sulfate polyacrylamide gel-electrophoresis
ETP	endogenous thrombin potential

REFERENCES

1. Fay PJ. Activation of factor VIII and mechanisms of cofactor action. Blood Rev. 2004; 18:1–15. [PubMed: 14684146]
2. Fay PJ. Reconstitution of human factor VIII from isolated subunits. Arch. Biochem. Biophys. 1988; 262:525–531. [PubMed: 3129993]
3. Wakabayashi H, Koszelak ME, Mastri M, Fay PJ. Metal ion-independent association of factor VIII subunits and the roles of calcium and copper ions for cofactor activity and inter-subunit affinity. Biochemistry. 2001; 40:10293–10300. [PubMed: 11513607]

NIH-PA Author Manuscript

NIH-PA Author Manuscript

NIH-PA Author Manuscript

4. Wakabayashi H, Freas J, Zhou Q, Fay PJ. Residues 110-126 in the A1 domain of factor VIII contain a Ca2+ binding site required for cofactor activity. J. Biol. Chem. 2004; 279:12677–12684. [PubMed: 14722121]
5. Wakabayashi H, Zhou Q, Nogami K, Ansong C, Varfaj F, Miles S, Fay PJ. pH-dependent association of factor VIII chains: enhancement of affinity at physiological pH by Cu2+ Biochim. Biophys. Acta. 2006; 1764:1094–1101. [PubMed: 16731058]
6. Ansong C, Fay PJ. Factor VIII A3 Domain Residues 1954-1961 Represent an A1 Domain-Interactive Site. Biochemistry. 2005; 44:8850–8857. [PubMed: 15952791]
7. Shen BW, Spiegel PC, Chang CH, Huh JW, Lee JS, Kim J, Kim YH, Stoddard BL. The tertiary structure and domain organization of coagulation factor VIII. Blood. 2008; 111:1240–1247. [PubMed: 17965321]
8. Ngo JC, Huang M, Roth DA, Furie BC, Furie B. Crystal structure of human factor VIII: implications for the formation of the factor IXa-factor VIIIa complex. Structure. 2008; 16:597–606. [PubMed: 18400180]
9. Fay PJ, Haidaris PJ, Smudzin TM. Human factor VIIIa subunit structure. Reconstruction of factor VIIIa from the isolated A1/A3-C1-C2 dimer and A2 subunit. J. Biol. Chem. 1991; 266:8957–8962. [PubMed: 1902833]
10. Lollar P, Parker CG. pH-dependent denaturation of thrombin activated porcine factor VIII. J. Biol. Chem. 1990; 265
11. Lollar P, Parker ET. Structural basis for the decreased procoagulant activity of human factor VIII compared to the porcine homolog. J. Biol. Chem. 1991; 266:12481–12486. [PubMed: 1905722]
12. Fay PJ, Beattie TL, Regan LM, O'Brien LM, Kaufman RJ. Model for the factor VIIIa-dependent decay of the intrinsic factor Xase. Role of subunit dissociation and factor IXa-catalyzed proteolysis. J. Biol. Chem. 1996; 271:6027–6032. [PubMed: 8626386]
13. Wakabayashi H, Fay PJ. Identification of Residues Contributing to A2 Domain-dependent Structural Stability in Factor VIII and Factor VIIIa. J. Biol. Chem. 2008; 283
14. Sammond DW, Eletr ZM, Purbeck C, Kimple RJ, Siderovski DP, Kuhlman B. Structure-based protocol for identifying mutations that enhance protein-protein binding affinities. J. Mol. Biol. 2007; 371:1392–1404. [PubMed: 17603074]
15. Wakabayashi H, Varfaj F, Deangelis J, Fay PJ. Generation of enhanced stability factor VIII variants by replacement of charged residues at the A2 domain interface. Blood. 2008; 112
16. Wakabayashi H, Griffiths AE, Fay PJ. Combining mutations of charged residues at the A2 domain interface enhances factor VIII stability over single point mutations. J. Thromb. Haemost. 2009; 7:438–444. [PubMed: 19067791]
17. Wakabayashi H, Griffiths AE, Fay PJ. Increasing hydrophobicity or disulfide bridging at the factor VIII A1 and C2 domain interface enhances procofactor stability. J. Biol. Chem. 2011; 286:25748–25755. [PubMed: 21628455]
18. Pipe SW, Kaufman RJ. Characterization of a genetically engineered inactivation-resistant coagulation factor VIIIa. Proc. Natl. Acad. Sci. U. S. A. 1997; 94:11851–11856. [PubMed: 9342326]
19. Gale AJ, Pellequer JL. An engineered interdomain disulfide bond stabilizes human blood coagulation factor VIIIa. J. Thromb. Haemost. 2003; 1:1966–1971. [PubMed: 12941038]
20. Mimms LT, Zampighi G, Nozaki Y, Tanford C, Reynolds JA. Phospholipid vesicle formation and transmembrane protein incorporation using octyl glucoside. Biochemistry. 1981; 20:833–840. [PubMed: 7213617]
21. Doering C, Parker ET, Healey JF, Craddock HN, Barrow RT, Lollar P. Expression and characterization of recombinant murine factor VIII. Thromb. Haemost. 2002; 88:450–458. [PubMed: 12353075]
22. Wakabayashi H, Su YC, Ahmad SS, Walsh PN, Fay PJ. A Glu113Ala Mutation within a Factor VIII Ca(2+)-Binding Site Enhances Cofactor Interactions in Factor Xase. Biochemistry. 2005; 44:10298–10304. [PubMed: 16042406]
23. Hemker HC, Giesen P, Al Dieri R, Regnault V, de Smedt E, Wagenvoord R, Lecompte T, Beguin S. Calibrated automated thrombin generation measurement in clotting plasma. Pathophysiol. Haemost. Thromb. 2003; 33:4–15. [PubMed: 12853707]

NIH-PA Author Manuscript

NIH-PA Author Manuscript

NIH-PA Author Manuscript

24. Ansong C, Miles SM, Fay PJ. Factor VIII A1 domain residues 97-105 represent a light chain-interactive site. Biochemistry. 2006; 45:13140–13149. [PubMed: 17073436]

25. Nogami K, Shima M, Hosokawa K, Suzuki T, Koide T, Saenko EL, Scandella D, Shibata M, Kamisue S, Tanaka I, Yoshioka A. Role of factor VIII C2 domain in factor VIII binding to factor Xa. J. Biol. Chem. 1999; 274:31000–31007. [PubMed: 10521497]

26. Ahmad SS, Walsh PN. Role of the C2 domain of factor VIIIa in the assembly of factor-X activating complex on the platelet membrane. Biochemistry. 2005; 44:13858–13865. [PubMed: 16229474]

27. Soeda T, Nogami K, Nishiya K, Takeyama M, Ogiwara K, Sakata Y, Yoshioka A, Shima M. The factor VIIIa C2 domain (residues 2228-2240) interacts with the factor IXa Gla domain in the factor xase complex. J. Biol. Chem. 2009; 284:3379–3388. [PubMed: 19047063]

NIH-PA Author Manuscript
NIH-PA Author Manuscript
NIH-PA Author Manuscript

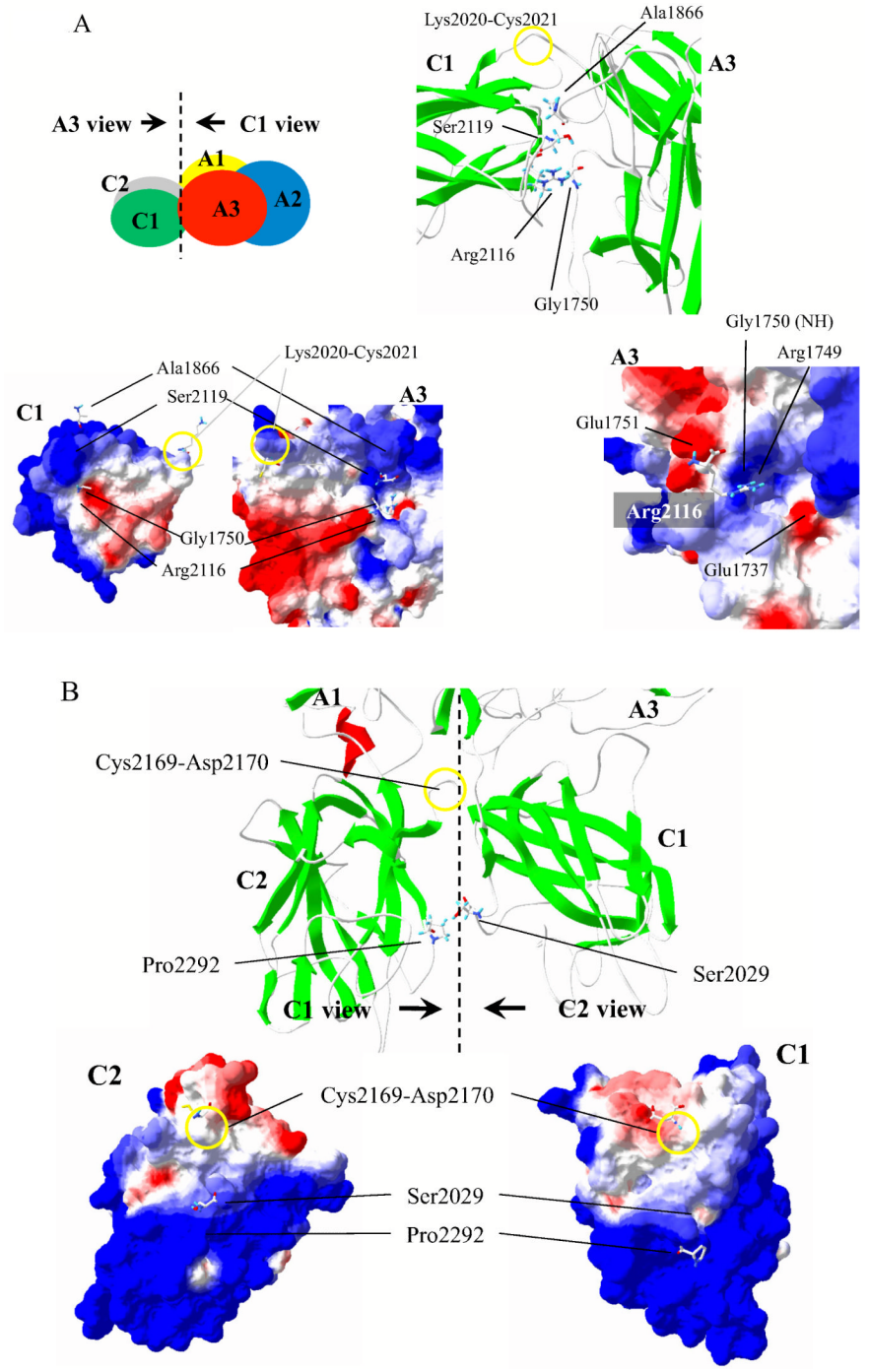

Figure 1.

(A). Interface structure with selected residues at the A3-C1 domain interface. Top left panel: The molecular surface of the FVIII X-ray crystal structure[8] was drawn by Swiss PDB viewer showing A1 domain (residues 1-336) in yellow, A2 domain (residues 373-711) in blue, A3 domain (residues 1690-2020) in red, C1 domain (residues 2021-2169) in green, and C2 domain (residues 2170-2332) in grey. Each molecular surface of the interface is viewed in the direction of the arrow and is shown in bottom left panel. Bottom left panel: Electrostatic potential was calculated by Swiss PDB viewer with a simple coulomb

NIH-PA Author Manuscript

NIH-PA Author Manuscript

NIH-PA Author Manuscript

interaction mode using a uniform dielectric constant (= 80) and shown as red (negative) and blue (positive). Residues facing A3 and C1 surfaces are drawn in stick representations. Top right panel: Higher magnification of the A3-C1 contact region drawn in ribbon structures. The covalent bond at Lys2020-Cys2021 is indicated by a yellow circle. Several indicated key residues are drawn in stick representations. Bottom right panel: Higher magnification of the A3 surface with electrostatic potential. Arg2116 from C1 is drawn in stick representation. (B) Interface structure with selected residues at the C1-C2 domain interface. Top panel: Higher magnification of the C1-C2 contact region in ribbon structures. The covalent bond at Cys2169-Asp2170 is indicated by yellow circle. Ser2029 and Pro2292 are drawn in stick representations. Each molecular surface of the interface is viewed in the direction of the arrow and is shown in bottom panel. Bottom panel: Molecular surface with electrostatic interaction of C1 (right) and C2 (left) are shown. Residues facing C1 and C2 surfaces are drawn in stick representations. In the stick models hydrogen, carbon, oxygen, nitrogen, and sulfur are colored as cyan, white, red, blue, and yellow, respectively. Ribbon structures represent α-helix (red) and β-strand (green).

NIH-PA Author Manuscript

NIH-PA Author Manuscript

NIH-PA Author Manuscript

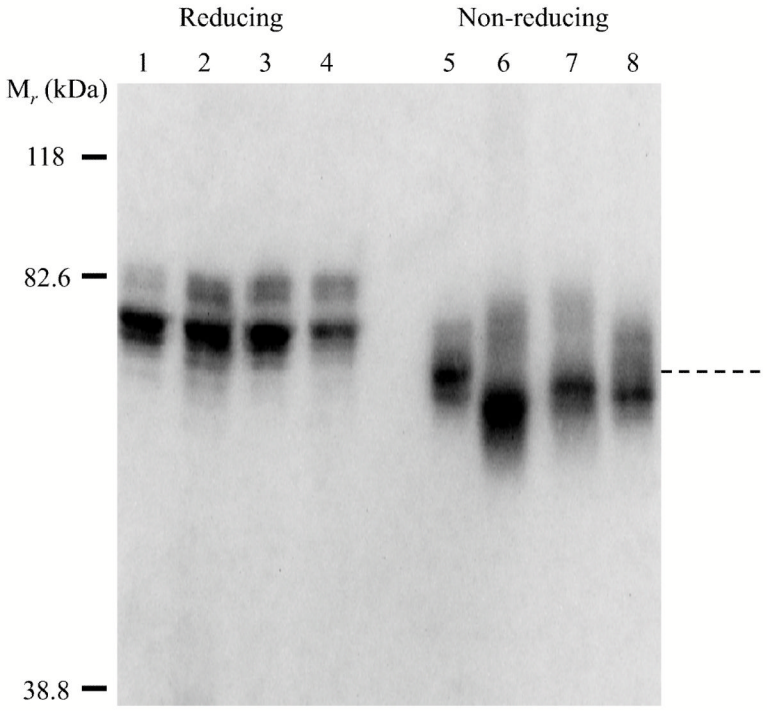

Figure 2.

Western blot analysis of WT FVIII and variants. Thrombin-activated WT and mutant FVIIIa proteins were electrophoresed under reducing (lanes 1-4) or non-reducing (lanes 5-8) conditions, transferred, and probed with 2D2 (anti-A3 domain monoclonal antibody). Protein bands were visualized by chemifluorescence as described in Methods. Shown are WT (lanes 1 and 5) Gly1750Cys/Arg2116Cys (lanes 2 and 6), Ala1866Cys/Ser2119Cys (lanes 3 and 7), and Ser2029Cys/Pro2292Cys (lanes 4 and 8) FVIII proteins.

NIH-PA Author Manuscript

NIH-PA Author Manuscript

NIH-PA Author Manuscript

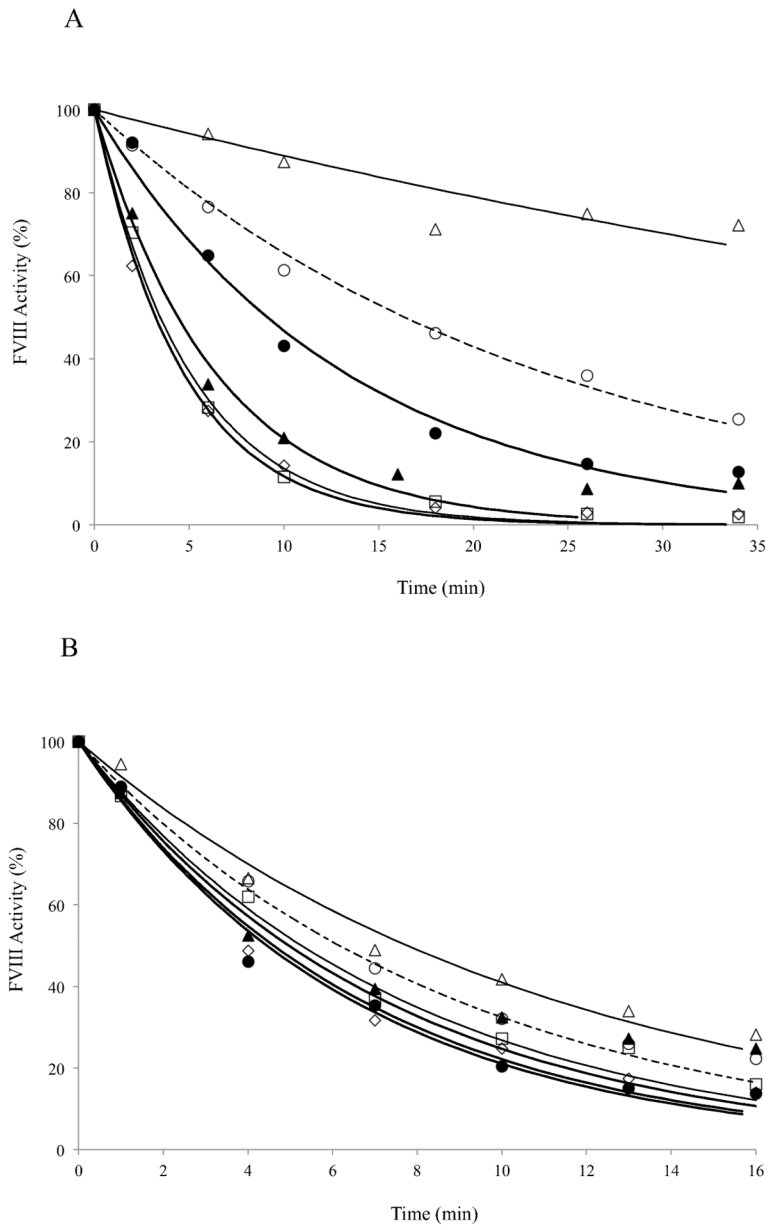

Figure 3.

(A) FVIII activity decay at elevated temperature. FVIII (4 nM) was incubated at 55°C and at the indicated times aliquots were removed and activity was measured by FXa generation assays as described in Methods. Data were fitted to a single exponential decay curve by non-linear least squares regression and lines were drawn. (B) FVIIIa decay. Thrombin-activated FVIIIa (1.5 nM) was incubated at 23°C, aliquots were taken at indicated time points and activity was measured by FXa generation assay as described in Methods. Data were fitted to a single exponential decay curve by non-linear least squares regression and lines were drawn. Symbols denote WT (open circles with dotted lines), Gly1750Cys/Arg2116Cys (open triangles), Ala1866Cys/Ser2119Cys (open squares), Arg2116Ala (open diamonds), Arg2116Val (closed circles), and Ser2029Cys/Pro2292Cys (closed triangles). Each point represents the value averaged from three separate determinations.

NIH-PA Author Manuscript

NIH-PA Author Manuscript

NIH-PA Author Manuscript

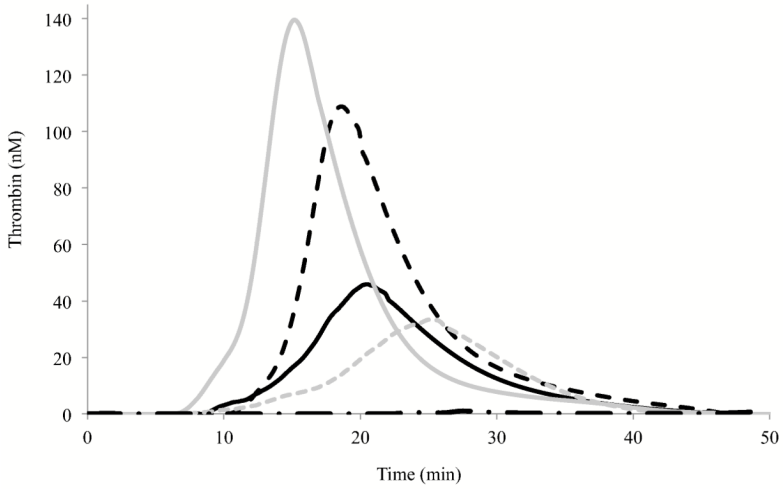

Figure 4.

Thrombin generation assay. Thrombin generation assays were performed in the presence of 0.25 nM FVIII WT or variant, 0.5 pM rTF, and 4 μM PSPCPE vesicles. Data represent the average values of triplicate samples. Representative thrombograms of WT (black dotted line), Gly1750Cys/Arg2116Cys (black solid line), Ala1866Cys/Ser2119Cys (grey dotted line), and Ser2029Cys/Pro2292Cys (grey solid line), and a negative control (0 nM FVIII, black alternate dash and dot line) are shown.

NIH-PA Author Manuscript
NIH-PA Author Manuscript
NIH-PA Author Manuscript

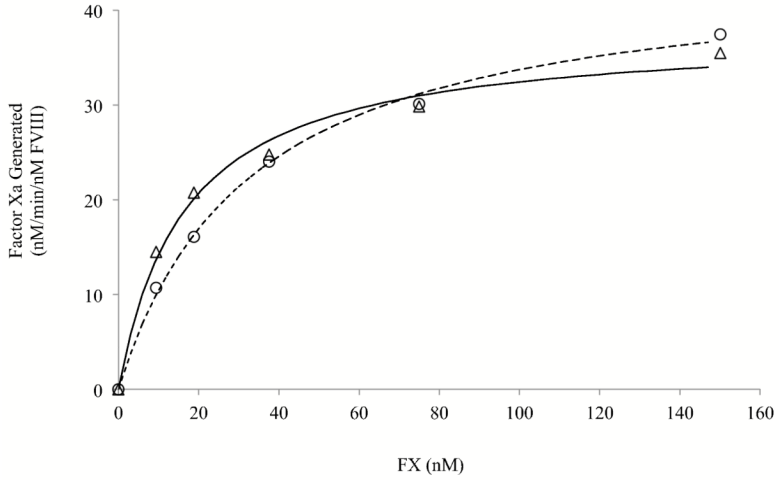

Figure 5.

Michaelis-Menten analysis of the FXase complex. FVIII (1 nM) was activated by 20 nM thrombin for 1 min, immediately reacted with hirudin (10 Unit/ml) and 40 nM FIXa, and FXa generation was initiated by adding the indicated concentrations of FX. The rate of generated FXa was measured as described in Methods. Data were fitted to Michaelis-Menten equation by non-linear least squares regression and fitted-lines were drawn. Each point represents the value averaged from three separate determinations. Symbols denote for WT (open circles) and Ser2029Cys/Pro2292Cys (open triangles).

NIH-PA Author Manuscript
NIH-PA Author Manuscript
NIH-PA Author Manuscript

Table 1

Factor VIII activity and stability data

	Clotting (U/μg)	FXa generation Assay (nM FXa/min/nM FVIII)	FVIII Decay Rate Constant (min^{-1})	FVIIIa Decay Rate Constant (min^{-1}) FIXa absent	FVIIIa Decay Rate Constant (min^{-1}) FIXa present
WT	4.61 ± 0.30 (1.00)	44.8 ± 0.8 (1.00)	0.0423 ± 0.0013 (1.00)	0.121 ± 0.012 (1.00)	0.018 ± 0.001 (1.00)
G1750C/R2116C	3.03 ± 0.11 (0.66)	26.1 ± 1.5 (0.58)	0.0118 ± 0.0014 (0.28)	0.089 ± 0.003 (0.74)	0.018 ± 0.001 (1.00)
A1866C/S2119C	1.37 ± 0.17 (0.30)	13.3 ± 0.8 (0.30)	0.1995 ± 0.0089 (4.71)	0.132 ± 0.004 (1.09)	0.019 ± 0.002 (1.06)
R2116A	4.81 ± 0.06 (1.04)	47.0 ± 1.3 (1.05)	0.2144 ± 0.0093 (5.07)	0.151 ± 0.008 (1.25)	0.017 ± 0.001 (0.94)
R2116V	4.04 ± 0.05 (0.88)	28.3 ± 0.5 (0.63)	0.0760 ± 0.0044 (1.80)	0.156 ± 0.009 (1.29)	0.018 ± 0.002 (1.00)
S2029C/P2292C	5.39 ± 0.10 (1.17)	37.8 ± 1.5 (0.85)	0.1572 ± 0.0118 (3.71)	0.140 ± 0.012 (1.16)	0.015 ± 0.001 (0.83)

FVIII activity by One-stage clotting and two-stage FXa generation assay and FVIII/FVIIIa stability by FVIII thermal activity decay at 55°C and FVIIIa spontaneous activity decay 23°C (in the presence or absence of FIXa) were measured as described in Methods. Activity and decay parameter values ± SD were calculated as described in Methods. Data represents the average values of triplicate samples. Values in parentheses are relative to the WT value. The single letter code is used to designate amino acid residues, G (Gly), R (Arg), A (Ala), S (Ser), C (Cys), V (Val), and P (Pro).

Biochemistry. Author manuscript; available in PMC 2014 June 04.

NIH-PA Author Manuscript
NIH-PA Author Manuscript
NIH-PA Author Manuscript

Table 2

Thrombin generation assay parameter values

	Latent Time (min)	Peak Time (min)	Peak Value (nM)	ETP (nM·min)
WT	11.9 ± 0.2 (1.00)	18.6 ± 0.1 (1.00)	108.9 ± 9.1 (1.00)	957.9 ± 41.1 (1.00)
G1750C/R2116C	11.5 ± 1.2 (0.97)	20.6 ± 1.0 (1.11)	45.9 ± 4.5 (0.42)	514.2 ± 19.7 (0.54)
A1866C/S2119C	13.2 ± 3.5 (1.11)	25.1 ± 2.7 (1.35)	33.4 ± 1.5 (0.31)	408.8 ± 36.5 (0.43)
R2116A	10.4 ± 0.2 (0.87)	18.2 ± 0.1 (0.98)	76.5 ± 8.6 (0.70)	744.1 ± 91.3 (0.78)
R2116V	12.6 ± 0.2 (1.06)	18.6 ± 0.1 (1.00)	69.4 ± 3.5 (0.64)	595.4 ± 4.4 (0.62)
S2029C/P2292C	7.8 ± 0.7 (0.66)	15.1 ± 0.3 (0.81)	139.6 ±12.8 (1.28)	1076.0 ± 24.0 (1.12)

Thrombin generation assays in the presence of 0.25 nM factor VIII proteins, 0.5 pM rTF, and 4 μM PSPCPE vesicles were performed and parameter values were calculated as described in Methods. Data represents the average values ± SD of triplicate samples. Values in parentheses are relative to the WT value. The single letter code is used to designate amino acid residues, G (Gly), R (Arg), A (Ala), S (Ser), C (Cys), V (Val), and P (Pro).